J. Fluid Mech. (1970), *vol.* 41, *part* 3, *pp.* 581–592
Printed in Great Britain

Cylindrical tank of fluid oscillating about a state of steady rotation

By CHANG-YI WANG

Department of Mathematics, University of California, Los Angeles†

(Received 19 May 1969)

A cylindrical tank, full of fluid, is oscillating with frequency ω and rotating with angular velocity Ω about its axis of symmetry. It is assumed that the amplitude of oscillation, δ, is small and the viscosity is low such that boundary layers exist. Analysis shows that the *unsteady* boundary layer is of thickness $[\epsilon/(1-2\Omega/\omega)]^{\frac{1}{2}}$ on the top and bottom plates and of thickness $\epsilon^{\frac{1}{2}}$ on the side walls, where $\epsilon = \nu/L^2\omega$. The interior unsteady flow shows source-like behaviour at the corners. The steady flow field is caused by the steady component of the non-linear centrifugal forces coupled with an induced steady rotation of the interior. This rotation, of order $\delta^2\omega$, is prograde when $\Omega/\omega < 0{\cdot}118$ and retrograde otherwise. Maximum retrograde rotation occurs at $\Omega/\omega = 0{\cdot}5$. A *steady* boundary layer of thickness $[\epsilon/(1-2\Omega/\omega)]^{\frac{1}{2}}$ exists on the top and bottom plates, and of thicknesses

$$\epsilon^{\frac{1}{2}}, \quad (\nu/L^2\Omega)^{\frac{1}{3}}, \quad (\nu/L^2\Omega)^{\frac{1}{4}}$$

on the side walls. Experimental measurements of the interior induced steady rotation compare well with theory.

1. Introduction

Oscillatory disturbances in a rotating fluid may be produced from primarily inviscid excitations, or from purely viscous effects. In the former case normal oscillations of the boundary push the fluid around, such as from a precessing non-spherical container, or from some oscillatory object inside the fluid. In the latter case an oscillating Ekman layer affects the interior by producing a time-dependent normal flux. It is well known, from linear theory, that inertial waves in the interior may be excited if the frequency of oscillation is smaller than twice the rotation rate of the fluid. See, for instance, Greenspan (1968). But are *non*-linear effects important for small amplitude disturbances?

For spin-up, Greenspan & Weinbaum (1965) showed that non-linear effects are unimportant. For small, steady precession of a spherical container, Busse (1968) showed that non-linear effects can produce a secondary retrograde motion of the interior, which is significant. In this paper we shall investigate the non-linear effects due only to small oscillatory disturbances.

Since inviscid excitation has secondary importance in producing non-linearities (Greenspan 1969), we shall study the case where purely viscous excitation is

† Present address: Department of Mathematics, Michigan State University, East Lansing, Michigan 48823.

dominant, i.e. torsional oscillation of a symmetric container about a state of steady rotation. To be specific, let us take a cylindrical tank, full of liquid of viscosity ν, of height L, radius αL, and rotating about its axis with the angular velocity $\Omega + \tilde{\Omega}\, e^{i\omega t}$, where α is a constant of unity, $\tilde{\Omega}$ and ω are the amplitude and frequency of oscillation respectively.

2. Analysis

Let us take a co-ordinate system rotating with angular velocity $\Omega\mathbf{k}$, where $\mathbf{k}$ is a unit vector. Then we separate the variables in the Navier–Stokes equations into a steady part denoted by a bar and an unsteady part denoted by a tilde:

$$\mathbf{q}' = \bar{\mathbf{q}}' + \tilde{\mathbf{q}}',$$
$$p' = \bar{p}' + \tilde{p}',$$

where $\mathbf{q}'$ is the velocity vector relative to the rotating system, and p' is the pressure plus the centrifugal potential due to Ω. Then we normalize the lengths by L, the time by $1/\omega$, $\bar{p}'$ by $\rho\tilde{\Omega}^2L^2$, $\tilde{p}'$ by $\rho\tilde{\Omega}\omega L^2$, the unsteady induced velocity $\tilde{\mathbf{q}}'$ by $\tilde{\Omega}L$, and the steady induced velocity $\bar{\mathbf{q}}'$ by $\bar{\Omega}L$, where the unknown magnitude $\bar{\Omega}$ shall be determined.

The Navier–Stokes equations then separate into an unsteady equation and a steady equation:

$$\tilde{\mathbf{q}}_t + \left(\frac{\bar{\Omega}}{\omega}\right)(\bar{\mathbf{q}}\cdot\nabla\tilde{\mathbf{q}} + \tilde{\mathbf{q}}\cdot\nabla\bar{\mathbf{q}}) + \left(\frac{\tilde{\Omega}}{\omega}\right)\widetilde{(\tilde{\mathbf{q}}\cdot\nabla\tilde{\mathbf{q}})} + \beta(2\mathbf{k}\times\tilde{\mathbf{q}}) = -\nabla\tilde{p} - \epsilon\nabla\times\nabla\times\tilde{\mathbf{q}}, \quad (2.1)$$

$$\left(\frac{\bar{\Omega}}{\tilde{\Omega}}\right)^2(\bar{\mathbf{q}}\cdot\nabla\bar{\mathbf{q}}) + \overline{(\tilde{\mathbf{q}}\cdot\nabla\tilde{\mathbf{q}})} + \beta\left(\frac{\bar{\Omega}\omega}{\tilde{\Omega}^2}\right)(2\mathbf{k}\times\bar{\mathbf{q}}) = -\nabla\bar{p} - \left(\frac{\epsilon\bar{\Omega}\omega}{\tilde{\Omega}^2}\right)\nabla\times\nabla\times\bar{\mathbf{q}}. \quad (2.2)$$

Here the unprimed quantities are of order unity, $\beta = \Omega/\omega$, $\epsilon = \nu/L^2\omega$, and $\widetilde{\ \ }$, $\overline{\ \ }$ denote the unsteady, steady part of the product respectively.

We assume the Stokes layer is small such that $\epsilon^{\frac{1}{2}} \ll 1$. We also assume the amplitude of oscillation is small such that

$$\tilde{\Omega}/\omega \ll \epsilon^{\frac{1}{2}} \ll 1.$$

Equation (2.1) shows that the unsteady velocity $\tilde{\mathbf{q}}$ decays within a distance of $\epsilon^{\frac{1}{2}}$ from the boundary. The prime motive force in (2.2) is the steady part of the Reynolds stress $\overline{(\tilde{\mathbf{q}}\cdot\nabla\tilde{\mathbf{q}})}$ which also decays in $\epsilon^{\frac{1}{2}}$. To balance this force in the same boundary-layer thickness, the induced velocity must have a magnitude such that $\bar{\Omega}/\omega = (\tilde{\Omega}/\omega)^2 \ll \epsilon \ll 1$.

Thus for the first two orders, the unsteady equation reduces to a linear problem, which, written in cylindrical polar co-ordinates becomes

$$\tilde{u}_t - 2\beta\tilde{v} = -\tilde{p}_r + \epsilon\left(\tilde{u}_{rr} + \frac{1}{r}\tilde{u}_r - \frac{\tilde{u}}{r^2} + \tilde{u}_{zz}\right), \quad (2.3)$$

$$\tilde{v}_t + 2\beta\tilde{u} = \epsilon\left(\tilde{v}_{rr} + \frac{1}{r}\tilde{v}_r - \frac{\tilde{v}}{r^2} + \tilde{v}_{zz}\right), \quad (2.4)$$

$$\tilde{w}_t = -\tilde{p}_z + \epsilon\left(\tilde{w}_{rr} + \frac{1}{r}\tilde{w}_r + \tilde{w}_{zz}\right). \quad (2.5)$$

The continuity equation is

$$(r\tilde{u})_r + (r\tilde{w})_z = 0. \tag{2.6}$$

Here u, v, w are the velocity components in the directions r, θ, z respectively. The boundary conditions are $\tilde{u} = \tilde{w} = 0$, $\tilde{v} = r\,e^{it}$ on top and bottom boundaries at $z = 0, 1$; $\tilde{u} = \tilde{w} = 0$, $\tilde{v} = \alpha\,e^{it}$ on the side walls at $r = \alpha$.

The bottom boundary-layer equations are obtained by stretching as follows

$$z = \epsilon^{\frac{1}{2}}\eta, \quad \tilde{\mathbf{q}} = \tilde{\mathbf{q}}_0 + \epsilon^{\frac{1}{2}}\tilde{\mathbf{q}}_1 + \ldots. \tag{2.7}$$

Equations (2.3)–(2.6) reduce to

$$\tilde{u}_{0t} - 2\beta\tilde{v}_0 = -\tilde{p}_{0r} + \tilde{u}_{0\eta\eta}, \tag{2.8}$$

$$\tilde{v}_{0t} + 2\beta\tilde{u}_0 = \tilde{v}_{0\eta\eta}, \tag{2.9}$$

$$\tilde{p}_{0\eta} = 0, \tag{2.10}$$

$$(r\tilde{u}_0)_r + (r\tilde{w}_0)_\eta = 0. \tag{2.11}$$

Solving these equations we obtain for the leading orders

$$\tilde{v}_0 = \tfrac{1}{2}r(G+F)\,e^{it}, \tag{2.12}$$

$$\tilde{w}_0 = 0, \tag{2.13}$$

$$\tilde{u}_0 = \tfrac{1}{2}ir(G-F)\,e^{it}, \tag{2.14}$$

$$\tilde{w}_1 = \frac{-(1+i)}{\sqrt{2}}\left[\frac{1-G}{(1+2\beta)^{\frac{1}{2}}} \mp \frac{1-F}{(1-2\beta)^{\frac{1}{2}}}\right]e^{it}, \tag{2.15}$$

where

$$G = \exp\left[-(1+2\beta)^{\frac{1}{2}}\frac{1+i}{\sqrt{2}}\eta\right], \tag{2.16}$$

$$F = \exp\left[\mp(1-2\beta)^{\frac{1}{2}}\frac{1+i}{\sqrt{2}}\eta\right]. \tag{2.17}$$

The top sign is used when $\beta < \frac{1}{2}$ and the bottom sign is used when $\beta > \frac{1}{2}$. We temporarily exclude the $\beta = \frac{1}{2}$ case. The solutions show the boundary layer is actually a combination of Stokes and Ekman layers. Its thickness is the Stokes thickness $\epsilon^{\frac{1}{2}}$ for small β and the Ekman thickness $(\epsilon/\beta)^{\frac{1}{2}} = E^{\frac{1}{2}}$ for large β. The top boundary layer has a similar construction.

The zeroth-order unsteady velocities in the interior are found to be zero. From (2.15) there is a mass flux of order $\epsilon^{\frac{1}{2}}$ into the interior. It is found that the side walls simply cannot support such large mass flux. To conserve mass, an unsteady source must exist near the corner of the tank. The first-order equation for the interior is

$$[(1/r)(r\tilde{\psi}_1)_r]_r + (1-4\beta^2)\,\tilde{\psi}_{1zz} = 0, \tag{2.18}$$

$$\tilde{V}_1 = -2\beta\tilde{\psi}_{1z}, \tag{2.19}$$

where ψ, related to the conventional stream function, is defined by

$$U = \psi_z, \quad W = -(1/r)(r\psi)_r. \tag{2.20}$$

The boundary conditions are that

$$\begin{aligned} &0 \leqslant r < \alpha, \quad z = 0, \quad \tilde{\psi}_1 = -\tfrac{1}{2}Ar\,e^{it}, \\ &\qquad z = \tfrac{1}{2}, \quad \tilde{\psi}_1 = 0, \\ &\qquad r = \alpha, \quad \tilde{\psi}_1 = 0, \\ &\qquad r = 0, \quad \tilde{\psi}_1 = 0, \end{aligned} \tag{2.21}$$

where $$A = -\frac{1+i}{\sqrt{2}}[(1+2\beta)^{-\frac{1}{2}} \mp (1-2\beta)^{-\frac{1}{2}}].$$

The solution to (2.18) plus the boundary conditions (2.21) can be obtained by separation of variables and a Fourier–Bessel expansion in r. The result is

$$\tilde{\psi}_1 = -A\alpha e^{it} \sum_{m=1}^{\infty} \frac{J_1(C_m r/\alpha)}{C_m J_2(C_m)} \frac{\sinh\left[\frac{C_m}{\alpha(1-4\beta^2)^{\frac{1}{2}}}(z-\frac{1}{2})\right]}{\sinh\left[\frac{-C_m}{2\alpha(1-4\beta^2)^{\frac{1}{2}}}\right]}, \tag{2.22}$$

where C_m is the mth positive zero of the Bessel function J_1. The velocity components are

$$\tilde{V}_1 = \frac{-2A\beta i e^{it}}{(1-4\beta^2)^{\frac{1}{2}}} \sum_{m=1}^{\infty} \frac{J_1(C_m r/\alpha)}{J_2(C_m)} \frac{\cosh\left[\frac{C_m}{\alpha(1-4\beta^2)^{\frac{1}{2}}}(z-\frac{1}{2})\right]}{\sinh\left[\frac{-C_m}{2\alpha(1-4\beta^2)^{\frac{1}{2}}}\right]}, \tag{2.23}$$

$$\tilde{W}_1 = A e^{it} \sum_{m=1}^{\infty} \frac{J_0(C_m r/\alpha)}{J_2(C_m)} \frac{\sinh\left[\frac{C_m}{\alpha(1-4\beta^2)^{\frac{1}{2}}}(z-\frac{1}{2})\right]}{\sinh\left[\frac{-C_m}{2\alpha(1-4\beta^2)^{\frac{1}{2}}}\right]}. \tag{2.24}$$

$\tilde{V}_1$ is an oscillatory azimuthal velocity in the interior, caused by the interaction of rotation with the oscillatory flux from the Ekman–Stokes layers near the top and bottom of the container. The vertical velocity $\tilde{W}_1$ is to be brought to rest in a side-wall boundary layer of order $\epsilon^{\frac{1}{2}}$ thickness.

On the side walls the variables are stretched as follows

$$\left.\begin{aligned} r &= \alpha - \epsilon^{\frac{1}{2}}\zeta, \\ \tilde{u} &= \epsilon\tilde{u}_2 + \ldots, \\ \tilde{v} &= \tilde{v}_0 + \ldots, \\ \tilde{w} &= \epsilon^{\frac{1}{2}}\tilde{w}_1 + \ldots, \\ \tilde{p} &= \epsilon^{\frac{1}{2}}\tilde{p}_1 + \ldots. \end{aligned}\right\} \tag{2.25}$$

Equations (2.3)–(2.6) reduce to

$$\left.\begin{aligned} -2\beta\tilde{v}_0 &= \tilde{p}_{1\zeta}, \\ i\tilde{v}_0 &= \tilde{v}_{0\zeta\zeta}, \\ i\tilde{w}_1 &= -\tilde{p}_{1z} + \tilde{w}_{1\zeta\zeta}, \\ \tilde{w}_{1z} &= \tilde{u}_{2\zeta}. \end{aligned}\right\} \tag{2.26}$$

The boundary conditions are

$$\zeta = 0, \quad \tilde{v}_0 = \alpha e^{it}, \quad \tilde{w}_1 = 0,$$
$$\zeta \to \infty, \quad \tilde{v}_0 \to 0, \quad \tilde{w}_1 \to \tilde{W}_1|_{r=\alpha}.$$

The solution is

$$\tilde{v}_0 = \alpha e^{it} \exp\left[-\frac{1+i}{\sqrt{2}}\zeta\right], \tag{2.27}$$

$$\tilde{w}_1 = A e^{it}\left\{1 - \exp\left[-\frac{1+i}{\sqrt{2}}\zeta\right]\right\} \sum_{m=1}^{\infty} \frac{J_0(C_m)}{J_2(C_m)} \frac{\sinh\left[\frac{C_m}{\alpha(1-4\beta^2)^{\frac{1}{2}}}(z-\frac{1}{2})\right]}{\sinh\left[\frac{-C_m}{2\alpha(1-4\beta^2)^{\frac{1}{2}}}\right]}. \tag{2.28}$$

There also exists a corner region, of dimensions $\epsilon^{\frac{1}{2}}$ by $[\epsilon/(1-2\beta)]^{\frac{1}{2}}$, where the mass flux of $\epsilon^{\frac{1}{2}}$ is redirected. This corner solution is difficult to obtain explicitly. The unsteady flow field is schematically shown in figure 1.

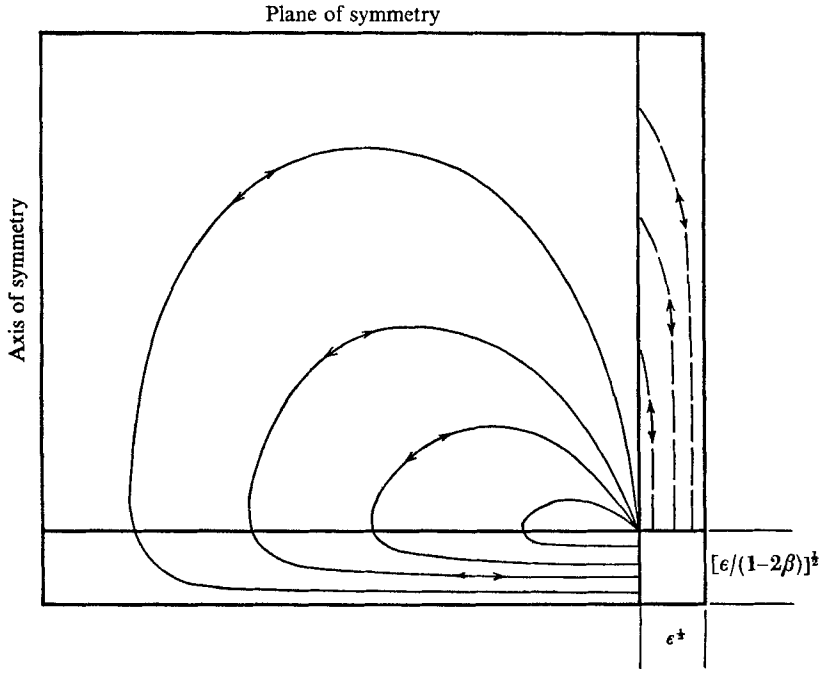

FIGURE 1. Schematic diagram of the *unsteady* flow field.
———, primary circulation; — — —, secondary circulation.

The steady flow induced by the unsteady velocities is strictly a non-linear phenomena. To second order, (2.2) becomes

$$\epsilon\left(\bar{u}_{rr}+\frac{1}{r}\bar{u}_r-\frac{\bar{u}}{r^2}+\bar{u}_{zz}\right)-\bar{p}_r+2\beta\bar{v}=\left(\overline{\tilde{u}\tilde{u}_r-\frac{\tilde{v}^2}{r}+\tilde{w}\tilde{u}_z}\right), \tag{2.29}$$

$$\epsilon\left(\bar{v}_{rr}+\frac{1}{r}\bar{v}_r-\frac{\bar{v}}{r^2}+\bar{v}_{zz}\right)-2\beta\bar{u}=\left(\overline{\tilde{u}\tilde{v}_r+\frac{\tilde{u}\tilde{v}}{r}+\tilde{w}\tilde{v}_z}\right), \tag{2.30}$$

$$\epsilon\left(\bar{w}_{rr}+\frac{1}{r}\bar{w}_r+\bar{w}_{zz}\right)-\bar{p}_z=(\overline{\tilde{u}\tilde{w}_r+\tilde{w}\tilde{w}_z}), \tag{2.31}$$

$$(r\bar{u})_r+(r\bar{w})_z=0. \tag{2.32}$$

The right-hand side represents the steady part of the Reynolds stress, mainly centrifugal forces, which decay exponentially to zero for the first two orders outside the boundary layer of order $\epsilon^{\frac{1}{2}}$. Thus the interior governing equations are

$$\left.\begin{aligned}-\overline{P}_r+2\beta\overline{V}&=0,\\-2\beta\overline{U}&=0,\\-\overline{P}_z&=0.\end{aligned}\right\} \tag{2.33}$$

If $\beta \neq 0$, (2.33) satisfies the Taylor–Proudman condition that,

$$\bar{U} \equiv 0, \tag{2.34}$$

$$\bar{V} = \bar{V}(r), \tag{2.35}$$

$$\bar{W} = \bar{W}(r) \equiv 0, \quad \text{by symmetry.} \tag{2.36}$$

From (2.7) and (2.29)–(2.32) the bottom boundary-layer equations are

$$\bar{u}_{0\eta\eta} + 2\beta\bar{v}_0 = \left(\overline{\tilde{u}_0\tilde{u}_{0r} - \frac{\tilde{v}_0^2}{r} + \tilde{w}_1\tilde{u}_{0\eta}}\right) + \bar{p}_{0r}$$

$$= rI(\eta) + 2\beta\bar{V}_0(r), \tag{2.37}$$

$$\bar{v}_{0\eta\eta} - 2\beta\bar{u}_0 = \left(\overline{\tilde{u}_0\tilde{u}_{0r} + \frac{\tilde{u}_0\tilde{v}_0}{r} + \tilde{w}_1\tilde{v}_{0\eta}}\right) = rJ(\eta), \tag{2.38}$$

$$(r\bar{u}_0)_r + (r\bar{w}_1)_\eta = 0. \tag{2.39}$$

Here $\bar{V}_0(r)$ is the steady azimuthal velocity of the interior, to be determined later, and

$$I(\eta) = \tfrac{1}{8}[B(\eta) + B^*(\eta)],$$

$$J(\eta) = \tfrac{1}{8}[C(\eta) + C^*(\eta)],$$

$$B(\eta) = \left(-2 + \frac{4\beta i}{(1-4\beta^2)^{\frac{1}{2}}}\right)GF^* + i\left(1 - \left(\frac{1+2\beta}{1-2\beta}\right)^{\frac{1}{2}}\right)G$$

$$\pm i\left(1 - \left(\frac{1-2\beta}{1+2\beta}\right)^{\frac{1}{2}}\right)F,$$

$$C(\eta) = \left(2i + \frac{4\beta}{(1-4\beta^2)^{\frac{1}{2}}}\right)GF^* - 2GG^* \pm 2FF^* + \left(1 - \left(\frac{1+2\beta}{1-2\beta}\right)^{\frac{1}{2}}\right)G$$

$$\mp\left(1 - \left(\frac{1-2\beta}{1+2\beta}\right)^{\frac{1}{2}}\right)F, \tag{2.40}$$

where the * denote the complex conjugate, and we bear in mind that

$$(1-2\beta)^{\frac{1}{2}*} = \pm(1-2\beta)^{\frac{1}{2}}.$$

The simplest way to solve for the steady flow is to define

$$\phi_0 = \bar{u}_0 - i\bar{v}_0. \tag{2.41}$$

Then (2.37)–(2.38) reduce to

$$\phi_{0\eta\eta} + 2i\beta\phi_0 = r(I - iJ) + 2\beta\bar{V}_0(r). \tag{2.42}$$

The boundary conditions are

$$\eta = 0, \quad \mathrm{Re}\,\phi_0 = 0, \quad \mathrm{Im}\,\phi_0 = 0. \tag{2.43}$$

After some algebra the solution is found to be

$$\phi_0 = \sum_{n=1}^{5} rK_n\{\exp(\alpha_n\eta) - \exp[-(1-i)\,\beta^{\frac{1}{2}}\eta]\} - i\bar{V}_0(r)\{1 - \exp[-(1-i)\,\beta^{\frac{1}{2}}\eta]\}, \tag{2.44}$$

where

$$\left.\begin{aligned}
\alpha_1 &= -2^{-\frac{1}{2}}[(1-i)(1+2\beta)^{\frac{1}{2}} \pm (1+i)(1-2\beta)^{\frac{1}{2}}],\\
\alpha_2 &= -2^{\frac{1}{2}}(1+2\beta)^{\frac{1}{2}},\\
\alpha_3 &= -2^{\frac{1}{2}}|1+2\beta|^{\frac{1}{2}},\\
\alpha_4 &= -\frac{1-i}{\sqrt{2}}(1+2\beta)^{\frac{1}{2}},\\
\alpha_5 &= \mp\frac{1+i}{\sqrt{2}}(1-2\beta)^{\frac{1}{2}},
\end{aligned}\right\} \tag{2.45}$$

$$\left.\begin{aligned}
K_1 &= \left(\tfrac{1}{4} \pm \frac{\beta i}{2(1-4\beta^2)^{\frac{1}{2}}}\right)(\beta i \mp (1-4\beta^2)^{\frac{1}{2}})^{-1},\\
K_2 &= \frac{i}{8(1+2\beta+i\beta)}, \qquad K_3 = \frac{\mp i}{8(|1-2\beta|+i\beta)},\\
K_4 &= \frac{1}{4}\left[1 \mp \left(\frac{1+2\beta}{1-2\beta}\right)^{\frac{1}{2}}\right], \quad K_5 = \pm\frac{1}{4}\left[1-\left(\frac{1-2\beta}{1+2\beta}\right)^{\frac{1}{2}}\right].
\end{aligned}\right\} \tag{2.46}$$

Similar to (2.20) we can define a steady stream function $\bar{\Psi}$ as follows

$$\bar{\Psi} = \int_0^z \bar{u}\,dz = \epsilon^{\frac{1}{2}}\int_0^\eta \operatorname{Re}\phi_0\,d\eta. \tag{2.47}$$

At infinity (2.47) reduces to

$$\eta\to\infty, \quad \bar{\Psi} = -\tfrac{1}{2}(\epsilon/\beta)^{\frac{1}{2}}[\bar{V}_0(r) - r\Omega'], \tag{2.48}$$

where

$$\Omega' = -\operatorname{Re}\sum_{n=1}^{5} K_n\left(\frac{2(\beta)^{\frac{1}{2}}}{\alpha_n}+1+i\right). \tag{2.49}$$

For boundary layers not close to the side walls, (2.36) implies the interior cannot take any mass flux. Equating (2.48) to zero, we find the interior fluid rotates rigidly as a whole

$$\bar{V}_0(r) = r\Omega'. \tag{2.50}$$

The angular velocity Ω' is plotted in figure 2. Taking limits on (2.49) we find $\beta\to 0$, $\Omega'\to\frac{1}{4}$; $\beta\to\frac{1}{2}$, $\Omega'\to -\frac{1}{34}(29\sqrt{2}-30)$; $\beta\to\infty$, $\Omega'\to -3/(20\beta)$. The stream function for the bottom boundary layer is then

$$\begin{aligned}
\bar{\Psi} = \epsilon^{\frac{1}{2}} r\Bigg\{ &\sum_{n=1}^{5} \operatorname{Re} K_n\left[\frac{\exp(\alpha_n\eta)}{\alpha_n} + \frac{1+i}{2\beta^{\frac{1}{2}}}\exp[-(1-i)\beta^{\frac{1}{2}}\eta]\right]\\
&-\operatorname{Re}\left[\sum_{n=1}^{5} K_n\left(\frac{2\beta^{\frac{1}{2}}}{\alpha_n}+1+i\right)\right]\operatorname{Re}\left[\frac{1-i}{2\beta^{\frac{1}{2}}}\exp[-(1-i)\beta^{\frac{1}{2}}\eta]\right]\Bigg\}.
\end{aligned} \tag{2.51}$$

On the side walls the steady azimuthal velocity $\bar{V}_0(r)$ must be brought to rest in an $E^{\frac{1}{4}} = (\epsilon/\beta)^{\frac{1}{4}}$ layer. This induces a mass flux that can only be balanced in an $E^{\frac{1}{3}}$ layer. For the $E^{\frac{1}{4}}$ layer the variables are stretched as follows

$$\left.\begin{aligned}
r &= \alpha - E^{\frac{1}{4}}\chi,\\
\bar{\Psi} &= E^{\frac{1}{2}}\bar{\Psi}_1 + \ldots,\\
\bar{v} &= \bar{v}_0 + \ldots.
\end{aligned}\right\} \tag{2.52}$$

Equations (2.20), (2.29)–(2.32) give

$$\left.\begin{aligned} \bar{v}_{0z} &= 0, \\ \bar{v}_{0\chi\chi} &= 2\bar{\Psi}_{1z}. \end{aligned}\right\} \tag{2.53}$$

The boundary conditions are

$$\left.\begin{aligned} z = \tfrac{1}{2}, &\quad \bar{\Psi}_1 = 0, \\ \text{from (2.48)}, \quad z = 0, &\quad \bar{\Psi}_1 = -\tfrac{1}{2}[\bar{v}_0(\alpha) - \alpha\Omega'], \\ \chi = 0, &\quad \bar{v}_0 = 0, \\ \text{from (2.50)}, \quad \chi \to \infty, &\quad \bar{v}_0 \to \alpha\Omega'. \end{aligned}\right\} \tag{2.54}$$

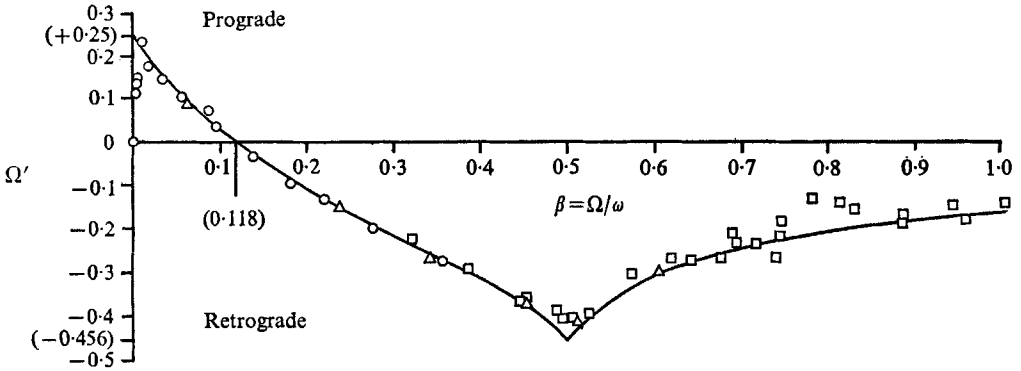

FIGURE 2. Induced steady rotation. ———, theory; ○, ω = 206 rev/min, δ = 15·5°; △, ω = 109 rev/min, δ = 15°; □, ω = 71 rev/min, δ = 16°.

The solution is

$$\bar{v} = \alpha\Omega'(1 - \exp[-\sqrt{2}\chi]) + \ldots, \tag{2.55}$$

$$\bar{\Psi} = -E^{\frac{1}{2}}\alpha\Omega' \exp[-\sqrt{2}\,\chi](z - \tfrac{1}{2}) + \ldots. \tag{2.56}$$

For the $E^{\frac{1}{3}}$ layer we set

$$\left.\begin{aligned} r &= \alpha - E^{\frac{1}{3}}\xi, \\ \bar{v} &= E^{\frac{1}{6}}\bar{v}_1 + \ldots, \\ \bar{\Psi} &= E^{\frac{1}{2}}\bar{\Psi}_1 + \ldots. \end{aligned}\right\} \tag{2.57}$$

The governing equations are

$$\bar{\Psi}_{1\xi\xi\xi\xi} + 2\bar{v}_{1z} = 0, \tag{2.58}$$

$$\bar{v}_{1\xi\xi} - 2\bar{\Psi}_{1z} = 0, \tag{2.59}$$

together with the boundary conditions

$$\left.\begin{aligned} z = \tfrac{1}{2}, &\quad \bar{\Psi}_1 = 0, \\ z = 0, &\quad \bar{\Psi}_1 = \tfrac{1}{2}\alpha\Omega', \\ \xi = 0, &\quad \bar{v}_1 = 0, \quad \bar{\Psi}_1 = 0, \\ \xi \to \infty, &\quad \bar{\Psi}_1 \to -\alpha\Omega'(z - \tfrac{1}{2}). \end{aligned}\right\} \tag{2.60}$$

The work involved is tedious but straightforward. We obtain

$$\bar{\Psi} = E^{\frac{1}{2}}\left[\sum_{n=1}^{\infty} \frac{(-1)^n \alpha\Omega'}{6\pi n}\{(3 + \sqrt{3}\,i)\exp[\tfrac{1}{2}\{-(4\pi n)^{\frac{1}{3}}\}(1 + \sqrt{3}\,i)\,\xi] + (3 - \sqrt{3}\,i)\exp[\tfrac{1}{2}\{-(4n\pi)^{\frac{1}{3}}\}(1 - \sqrt{3}\,i)\,\xi]\}\sin n\pi(1 - 2z) - \alpha\Omega'(z - \tfrac{1}{2})\right]. \tag{2.61}$$

The velocity $\bar{v}_1$ again induces an $E^{\frac{1}{3}}$ azimuthal velocity into the $E^{\frac{1}{4}}$ layer, but this is of lesser importance.

Close to the wall, there is an $\epsilon^{\frac{1}{4}}$ layer where the right-hand side of (2.29)–(2.31) is important. These terms will change the steady radial pressure distribution. The velocities will not be affected except in the corner region of dimensions $\epsilon^{\frac{1}{2}}$ by $[\epsilon/(1-2\beta)]^{\frac{1}{2}}$.

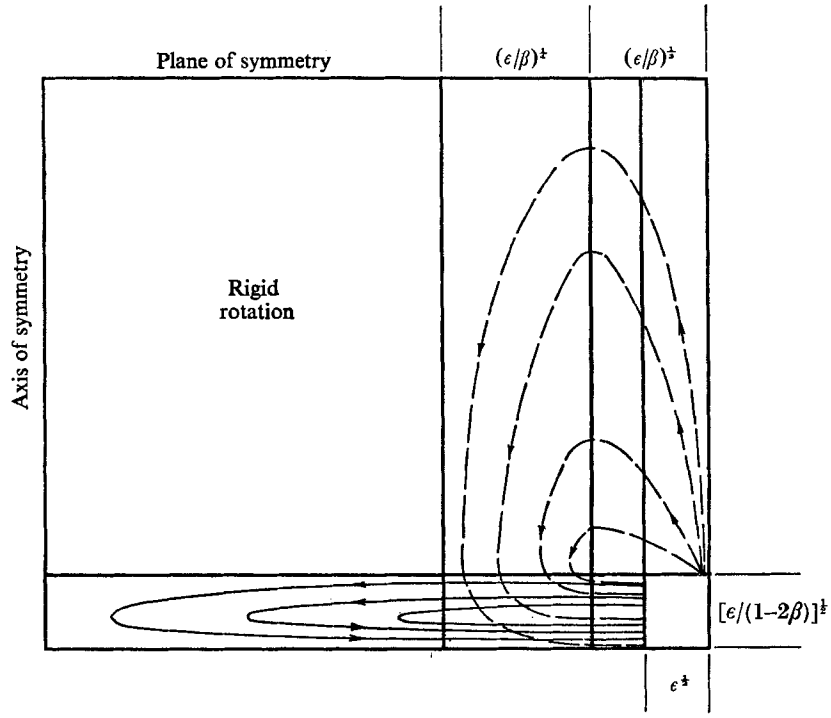

FIGURE 3. Schematic diagram of the *steady* flow field. ———, bottom boundary-layer circulation; — — —, side wall boundary-layer circulation.

Figure 3 shows the various boundary-layer thicknesses encountered in the steady flow. The scale of this figure is drawn such that β is of order unity or lower and not close to $\frac{1}{2}$. Other distributions of the regions are possible when β is large or close to $\frac{1}{2}$, e.g.

$$\epsilon^{\frac{1}{2}} \sim (\epsilon/\beta)^{\frac{1}{3}}, \quad \text{or} \quad [\epsilon/(1-2\beta)]^{\frac{1}{2}} \sim (\epsilon/\beta)^{\frac{1}{4}}.$$

The basic mechanism for steady flow, however, is similar.

3. Experiments

Experiments were done to detect the steady rotation of the interior due to non-linear effects caused by oscillation. A cylindrical tank, of $10\frac{5}{8}$ in. diameter and 12 in. height was filled with water at room temperature. A free-supported vaned shaft was placed along the axis of the cylinder. Near the tip of the shaft, which protruded out through a hole on the cylinder, was attached a small slitted disk. A photocell sandwiches part of the disk and records its angular velocity.

The tank of fluid was able to oscillate through a crank-and-rocker mechanism driven by a motor. The amplitude of oscillation δ, was about 15·5°. The whole apparatus rested on a variable speed turntable (figure 4, plate 1).

The turntable was run at a fixed angular velocity while the cylinder was made to oscillate. After all transients died out, the steady induced angular velocity of the interior was picked up by the photocell and recorded. The results show good agreement with theory calculated from (2.50). See figure 2.

The magnitude of the induced steady flow is of order $\tilde{\Omega}^2/\omega = \frac{1}{4}\delta^2\omega$; it is proportional to the frequency of oscillation ω and the square of the amplitude of oscillation δ. The rotation is *prograde* for $\beta < 0{\cdot}118$ and *retrograde* for $\beta > 0{\cdot}118$. For β near zero, theory shows Ω' approach the maximum prograde value of $+0{\cdot}25$, while experimental values rise sharply from zero to the theoretical value. This is because in the experiments the rotation rate is too slow for an effective Taylor column to establish. At $\beta = \frac{1}{2}$ theory shows the induced rotation approaches the limit $\Omega' = -0{\cdot}456$ which is the maximum retrograde angular velocity. It seems, as far as the induced steady motion is concerned, consideration of the $\beta \approx \frac{1}{2}$ case only amounts to rounding the cusp there, which is hardly worth the effort of introducing the necessary additional non-linear terms into (2.8)–(2.9).

For $\beta > \frac{1}{2}$ experiments show greater scatter as compared with those of $\beta < \frac{1}{2}$. Numerous inviscid inertial waves may be excited in this range. The inertial oscillations, though unsteady, may produce a non-linear higher order steady component by interacting with the vanes in the tank. This effect would be minimized if the vanes are made perfectly symmetric. Nevertheless, we see that the general trend of experimental values follows the theoretical prediction.

4. Discussions

Benny (1965) was first to consider the Ekman–Stokes layer by studying an infinite disk which is rotating and oscillating in its own plane. He found that on the disk the boundary-layer thickness arises from the combination of the Ekman thickness and the Stokes thickness: $[\epsilon/(1 \pm 2\beta)]^{\frac{1}{2}}$. Benny further went on to show, due to non-linear centrifugal effects, that in the limit of $\beta \to 0$ there is a weak steady influx proportional to β into the boundary layer, and constant outfluxes occur when $\beta \to \frac{1}{2}$ and $\beta \to \infty$. Unfortunately, no details were given.

In our case, the presence of a similar symmetric top disk prevents any flux from leaving the boundary layer into the interior. The interior thus adjusts itself to force a much stronger Ekman flux which just balances the flux due to non-linear steady streaming caused by centrifugal forces.

Figure 5 shows the steady circulation of the bottom boundary layer calculated from (2.51). For small β the horizontal velocity reverses once, while for large β, there are two reversals in velocity. Conceptually, let us separate the Stokes layer from the Ekman layer. As $\beta \to 0$ the Ekman thickness $(\nu/\Omega)^{\frac{1}{2}}$ is much larger than the Stokes thickness $(\nu/\omega)^{\frac{1}{2}}$ which is closer to the boundary. The fluid in the Stokes layer is being thrown out due to centrifugal forces. Since it is bounded at the bottom by the solid plate, to conserve mass, fluid must be drawn from the Ekman layer above. To balance this downward flux, the interior must attain

a prograde motion. Therefore the fluid flows radially inwards in the Ekman layer and radially outward in the Stokes layer.

On the other hand, for large β we can imagine a thick Stokes layer which is lying on top of a thinner Ekman layer. Again inside the Stokes layer fluid is being thrown out. Since it is bounded from above by the interior, the mass flux must be replenished from below. The interior induced rotation, which only

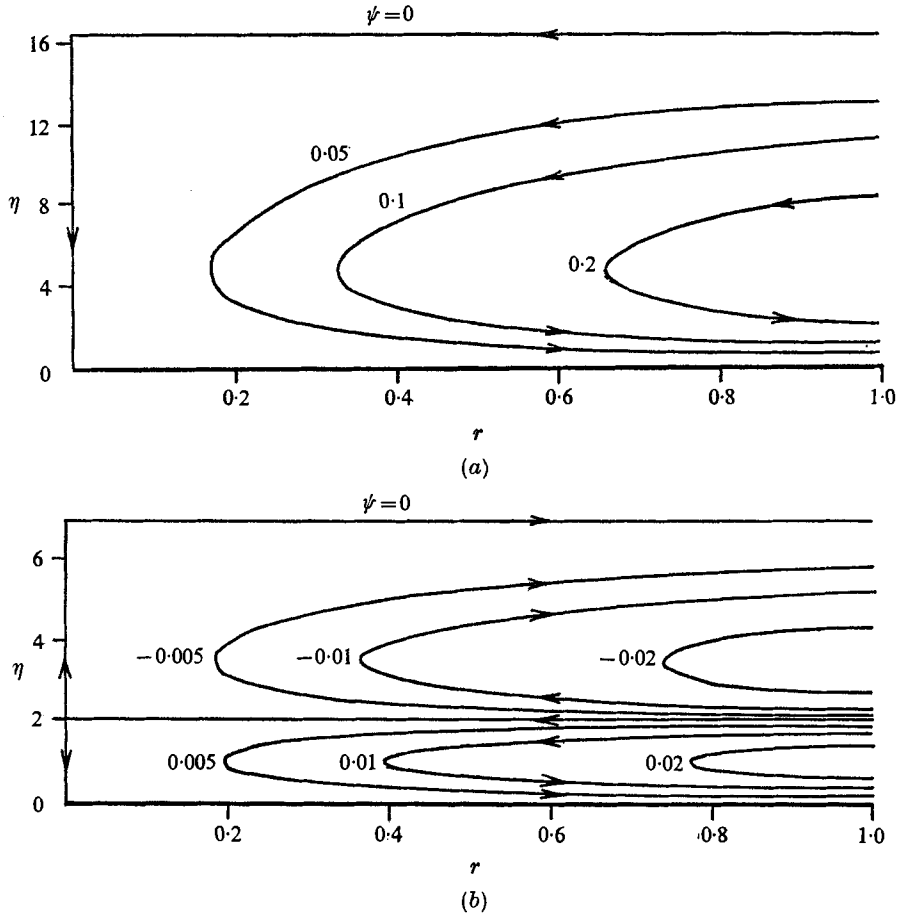

FIGURE 5. Steady circulations of the Ekman–Stokes layer. (*a*) $\beta = 0{\cdot}04$, (*b*) $\beta = 0{\cdot}9$.

affects the Ekman layer, must be retrograde in order to bring the upward flux to zero on the solid plate. There exists, however, a third 'layer' very near the oscillating plate where the outward centrifugal force reaches its maximum but the inward pressure due to the Ekman layer drops to zero. Thus we expect another outward flux very near the boundary.

For intermediate values of β the induced interior rotation depends on the delicate balance of the Ekman and the Stokes layers which is now of same order and highly coupled. What we can say is at $\beta \approx \frac{1}{2}$ the unsteady boundary-layer thickness reaches a maximum. The centrifugal force and thus the induced interior rotation would also reach a maximum for a fixed amplitude of oscillation.

The side walls only affect the unsteady flow field in the interior and have little effect on the induced steady rotation. For other geometries such as a sphere, we expect the steady rotation to vary continuously with radius. As the slope of the container gets steeper, the rotation gradually reaches a maximum retrograde motion at the 'critical layer', where, according to our theory, only a *finite* jump in the *derivative* of rotation rate is observed. This is quite different from Busse's work on precession, where the rotation rate itself goes through a *dipole* singularity.

Of less importance is the induced unsteady flow of frequency 3ω which is of the same order as the induced steady flow. Also we shall not go into the important resonant frequencies due to linear excitation of the inertial waves when $\beta > \frac{1}{2}$. These have been investigated by Fultz (1959) for the case of a cylinder, Greenspan (1964), Aldridge & Toomre (1969) for the case of a sphere. Both theoretical and experimental determinations of the eigenvalues agree very well.

This research was supported in part by Office of Naval Research contract number NONR 233(76). The author is grateful to Professor L. N. Howard and Professor W. V. R. Malkus for their many helpful discussions on both theory and experiment. The permission to use the facilities of the Geophysics Laboratory of the Institute of Geophysics and Planetary Physics at UCLA was also appreciated.

REFERENCES

ALDRIDGE, K. D. & TOOMRE, A. 1969 Axisymmetric inertial oscillations of a fluid in a rotating spherical container. *J. Fluid Mech.* **37**, 307–323.

BENNY, D. J. 1965 The flow induced by a disk oscillating about a steady state of rotation. *Quart. J. Mech. Appl. Math.* **18**, 333–345.

BUSSE, F. H. 1968 Steady fluid flow in a precessing spheroidal shell. *J. Fluid Mech.* **33**, 739–751.

FULTZ, D. 1959 A note on overstability and the elastoid-inertia oscillations of Kelvin, Solberg and Bjerkness. *J. Meteorol.* **16**, 199–208.

GREENSPAN, H. P. 1964 On the transient motion of a contained rotating fluid. *J. Fluid Mech.* **20**, 673–696.

GREENSPAN, H. P. 1968 *The Theory of Rotating Fluids.* Cambridge University Press.

GREENSPAN, H. P. 1969 On the non-linear interaction of inertial modes. *J. Fluid Mech.* **36**, 257–264.

GREENSPAN, H. P. & WEINBAUM, S. 1965 On non-linear spin-up of a rotating fluid. *J. Math. and Phys.* **44**, 66–85.

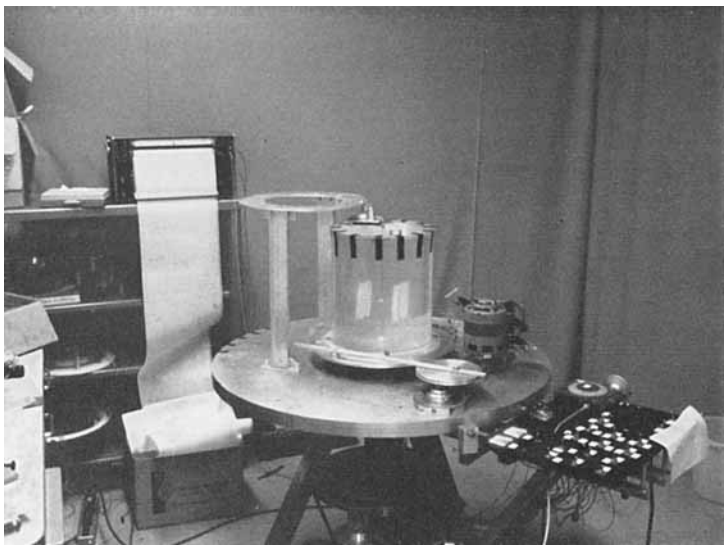

FIGURE 4. The experimental set up.